Chapter 8
Propagation and Polarization Characteristics of Single-Mode Fibers

8.1 Introduction

The invention of the laser in 1960 revolutionized the area of telecommunications, as it made it possible to modulate light waves at high frequencies. Initially, modulated laser beams propagating through open space were used to transmit information from one place to another. However, due to environmental disturbances, such as rain, fog, dust, temperature variations, and so on, such a transmission system was neither convenient nor reliable to use. Present-day optical communication systems use optical fibers through which information is transmitted in the form of optical pulses from one place to another. In the following, we discuss the basic propagation characteristics of optical fibers.

An *optical fiber* is a cylindrical structure, and the simplest (and the most extensively used) optical fiber is the *step-index fiber*, in which the refractive index distribution (in the transverse direction) is given by

$$n = \begin{cases} n_1 & 0 < r < a \\ n_2 & r > a, \end{cases} \tag{8.1}$$

where n_1 and n_2 ($< n_1$) represent the refractive indices of the core and the cladding, respectively, and a represents the radius of the core (see Fig. 8.1).

The cladding is usually pure silica, while the core is usually silica doped with germanium; doping by germanium results in an increase in refractive index. The guidance of the light beam (through the optical fiber) takes place because of the total internal reflection at the core–cladding interface. The rays for which the angle ϕ is more than the critical angle ϕ_c, where

$$\phi_c = \sin^{-1}\left(\frac{n_2}{n_1}\right) \tag{8.2}$$

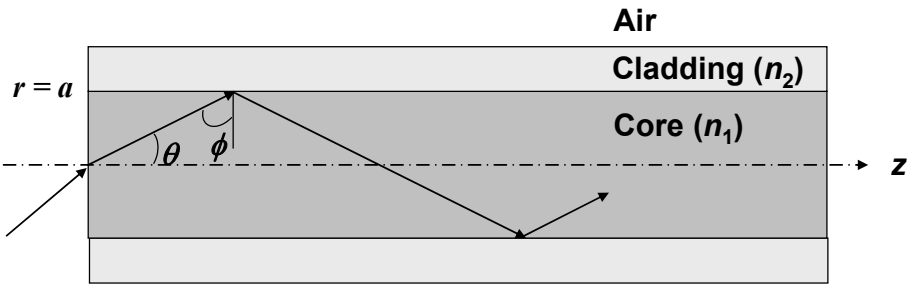


Figure 8.1 A step-index fiber. Light guidance takes place through the phenomenon of total internal reflection at the core–cladding interface.

will be totally internally reflected and will be guided through the core. The preceding condition of guidance can also be put in terms of angle θ made by the ray with the fiber axis. For guided rays,

$$\theta \leq \cos^{-1}\left(\frac{n_2}{n_1}\right). \tag{8.3}$$

When a light pulse propagates through an optical fiber, it suffers from attenuation due to various mechanisms, and the pulse broadens in time, leading to what is termed *pulse*/*chromatic dispersion*. Attenuation and chromatic dispersion represent the two most important characteristics that determine the information transmission capacity of optical fibers. Obviously, the lower the attenuation (and similarly, the lower the dispersion), the greater will be the required repeater spacing and therefore the higher the information-carrying capacity and the lower the cost of the communication system.

8.2 Attenuation in Optical Fibers

The attenuation in an optical fiber is specified in terms of the unit dB/km and is defined as

$$\alpha\ (\text{dB/km}) = \frac{10}{L\ (\text{km})} \log_{10}\left(\frac{P_{\text{in}}}{P_{\text{out}}}\right). \tag{8.4}$$

Here P_{in} and P_{out} are the input and output powers corresponding to an optical fiber of length L (km). The losses are caused by various mechanisms, such as Rayleigh scattering, absorption due to metallic impurities, and the presence of a small amount of water, as well as due to the intrinsic absorption of silica molecules. Even 1 part per million (ppm) of iron can cause a loss of about 0.68 dB/km at 1100 nm. Similarly, a concentration of 1 ppm of OH^- ion can cause a loss of 4 dB/km at 1380 nm. This shows the level of purity that is required to

achieve very low-loss optical fibers. The peaks shown in Fig. 8.2 are due to a very minute presence of OH^- ions as well as to metal impurities.

The lowest loss (~ 0.25 dB/km) occurs at about 1550 nm (the approximate wavelength[1] of erbium-doped fiber amplifiers); therefore, most optical communication systems today operate at this wavelength.

8.3 Modes of a Step-Index Fiber

In Section 8.1 we used ray optics to study propagation of a lightwave through a step-index fiber; however, this description is only approximate and cannot be used to understand the polarization characteristics of an optical fiber. The exact approach is to obtain the solutions of Maxwell's equations that satisfy the proper boundary conditions at the core–cladding interface, which are known as the *modes* of the optical fiber. The boundary conditions are the continuity of (i) the tangential components of **E** and **H**, and (ii) the normal components of **B** and **D** vectors at $r = a$. Physically, the modes are various transverse field distributions that propagate along the fiber without any change in their transverse field distributions.

The exact vector modes of optical fibers are a bit complicated, and their mathematical description is difficult. A system engineer who has not gone through a rigorous course on the theory of optical fibers will find it difficult to

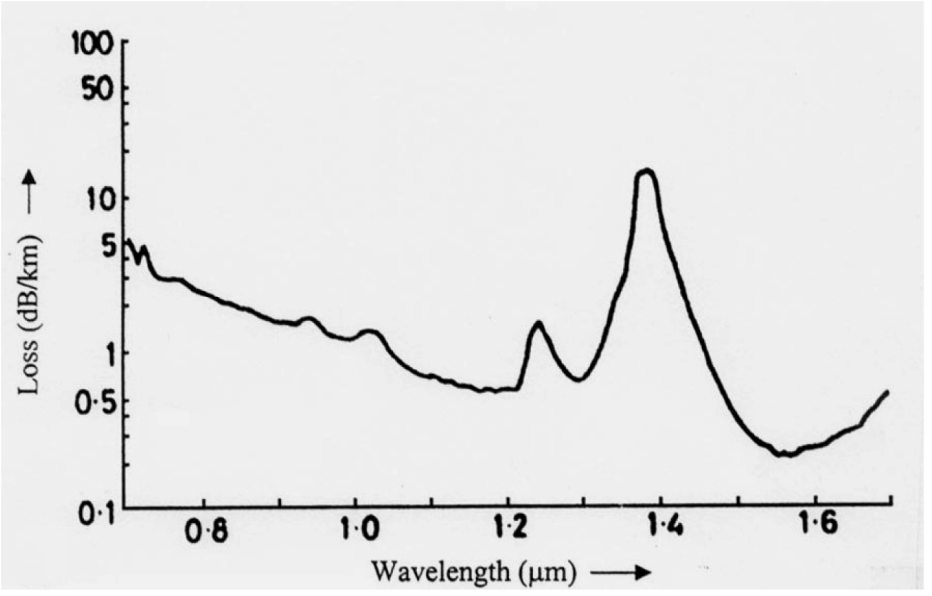


Figure 8.2 Typical wavelength dependence of loss for a silica fiber. The peaks in the attenuation curve in the wavelength regions 1.25 and 1.40 μm are due to the presence of minute amounts of water and other impurities. Notice that the lowest loss occurs at 1550 nm. (Reprinted with permission from Ref. 1, © 1979, IEEE.)

understand these modes. Fortunately, for practical single-mode fibers, the core and cladding refractive index difference $n_1 - n_2$ is extremely small, and one can use the weakly guiding approximation ($n_1 \approx n_2$) to obtain the propagation constants of the various modes, which makes the calculations extremely simple.

This approximation is also expressed in terms of a parameter Δ, defined as

$$\Delta \equiv \frac{n_1^2 - n_2^2}{2n_1^2}. \tag{8.5}$$

For $n_1 \approx n_2$, $\Delta << 1$, and

$$\Delta = \frac{n_1 - n_2}{n_1}\frac{n_1 + n_2}{2n_1} \approx \frac{n_1 - n_2}{n_2} \approx \frac{n_1 - n_2}{n_1}. \tag{8.6}$$

The error introduced by the weakly guiding approximation in the calculation of fiber modes is so small that in practice, the exact modes are rarely used. In this approximation, the modes of a fiber are linearly polarized and are known as linearly polarized (LP) modes, which are discussed in the following.

8.3.1 Linearly polarized (LP) modes

As discussed in Chapter 2, the solutions to Maxwell's equations in an infinitely extended homogeneous medium are transverse in nature and linearly polarized. In the weakly guiding approximation, $n_1 \approx n_2$, we assume that the modes of an optical fiber maintain the previously mentioned nature. Accordingly, we assume that the transverse component of the electric field (E_x or E_y) satisfies the following scalar wave equation:

$$\nabla^2 \Psi = \frac{n^2}{c^2}\frac{\partial^2 \Psi}{\partial t^2}, \tag{8.7}$$

where Ψ represents E_x (or E_y). Further, instead of satisfying the exact boundary conditions (continuity of E_z, $n^2 E_r$, and E_ϕ at $r = a$), we satisfy the continuity of E_x (or E_y) and $\partial E_x/\partial r$ (or $\partial E_y/\partial r$ at $r = a$. We solve Eq. (8.7) in the cylindrical system of coordinates and write the solution of Eq. (8.7) in the form

$$\Psi(r, \phi, z, t) = \psi(r, \phi) e^{i(\omega t - \beta z)}, \tag{8.8}$$

where β is the propagation constant.

Substituting Ψ from Eq. (8.8) into Eq. (8.7), one can easily show that $\psi(r,\phi)$ satisfies the following equation:

$$\frac{\partial^2\psi}{\partial r^2}+\frac{1}{r}\frac{\partial\psi}{\partial r}+\frac{1}{r^2}\frac{\partial^2\psi}{\partial\phi^2}+\left[k_0^2n^2(r)-\beta^2\right]\psi=0. \tag{8.9}$$

Equation (8.9) can be solved by using the method of separation of variables, i.e., $\psi(r,\phi)$ can be assumed to be of the form

$$\psi(r,\phi) = R(r)\Phi(\phi). \tag{8.10}$$

Substituting $\psi(r,\phi)$ from Eq. (8.10) into Eq. (8.9), one obtains

$$\frac{r^2}{R}\left(\frac{d^2R}{dr^2}+\frac{1}{r}\frac{dR}{dr}\right)+r^2\left[k_0^2n^2(r)-\beta^2\right]=-\frac{1}{\Phi}\frac{\partial^2\Phi}{\partial\phi^2} = l^2, \tag{8.11}$$

where l is a constant. Since the medium has cylindrical symmetry, the ϕ dependence of $\psi(r,\phi)$ should be of the form $\cos l\phi$ or $\sin l\phi$, and for the function to be single-valued, i.e., $\Phi(\phi+2\pi)=\Phi(\phi)$, we must have l = 0, 1, 2, …. Thus, $\psi(r,\phi)$ is given by

$$\psi(r,\phi) = R(r)\begin{Bmatrix}\cos l\phi\\ \sin l\phi\end{Bmatrix}, \tag{8.12}$$

where $R(r)$ satisfies the radial part of Eq. (8.9):

$$r^2\frac{d^2R}{dr^2}+r\frac{dR}{dr}+\left\{\left[k_0^2n^2(r)-\beta^2\right]\ r^2-l^2\right\}R=0. \tag{8.13}$$

Before we solve Eq. (8.13), we will make some general comments about its solutions, which can be divided into two distinct classes:

(i) *Guided modes*: For guided modes,

$$k_0n_2<\beta<k_0n_1. \tag{8.14}$$

For β lying in the preceding range, the field $R(r)$ is oscillatory in the core and decays in the cladding, and β assumes only discrete values; these are known as the *guided modes* of the waveguide. For a given value of l, there will be several guided modes.

(ii) *Radiation modes*: For radiation modes, $\beta < k_0 n_2$, the fields are oscillatory in the core as well as cladding, and β can assume a continuum of values. These are known as the *radiation modes.* Such modes leak away quickly and hence are not important in a long-distance communication system. In the analysis provided in this section, we will concentrate only on the guided modes.

For a step-index fiber, the well-behaved solutions of Eq. (8.13), which are continuous at the $r = a$ interface, can be written in terms of Bessel functions[2–4] J_l and K_l as

$$R(r) = \begin{cases} \dfrac{A}{J_l(U)} J_l\left(\dfrac{Ur}{a}\right) & r < a \\ \dfrac{A}{K_l(W)} K_l\left(\dfrac{Wr}{a}\right) & r > a. \end{cases} \tag{8.15}$$

Thus,

$$\psi(r,\phi) = \begin{cases} \dfrac{A}{J_l(U)} J_l\left(\dfrac{Ur}{a}\right) \begin{bmatrix} \cos l\phi \\ \sin l\phi \end{bmatrix} & r < a \\ \dfrac{A}{K_l(W)} K_l\left(\dfrac{Wr}{a}\right) \begin{bmatrix} \cos l\phi \\ \sin l\phi \end{bmatrix} & r > a, \end{cases} \tag{8.16}$$

where A is a constant, and we have assumed the continuity of ψ at the core–cladding interface. The constants U and W are defined as

$$U = a\sqrt{k_0^2 n_1^2 - \beta^2} \text{ and } W = a\sqrt{\beta^2 - k_0^2 n_2^2}\ . \tag{8.17}$$

For guided modes, $n_2^2 k_0^2 < \beta^2 < n_1^2 k_0^2$, and therefore, both U and W are real.

The normalized waveguide parameter V is defined as

$$V = \sqrt{U^2 + W^2} = k_0 a\sqrt{n_1^2 - n_2^2}\ . \tag{8.18}$$

The waveguide parameter V (which also depends on the operating wavelength λ_0) is an extremely important quantity characterizing an optical fiber.

If we make $d\psi / dr$ continuous at $r = a$, we obtain the eigenvalue equation for LP modes as

$$\frac{UJ_l'(U)}{J_l(U)} = \frac{WK_l'(W)}{K_l(W)}, \tag{8.19}$$

where $J_l'(U)$ and $K_l'(W)$ represent the derivatives of $J_l(U)$ and $K_l(W)$ with respect to their arguments. Using the following recurrence relations of Bessel functions:

$$J_l'(x) = \mp \frac{lJ_l(x)}{x} \pm J_{l\mp1}(x) \tag{8.20a}$$

$$K_l'(x) = \mp \frac{lK_l(x)}{x} - K_{l\mp1}(x), \tag{8.20b}$$

Eq. (8.19) can be recast as

$$\frac{UJ_{l-1}(U)}{J_l(U)} = -\frac{WK_{l-1}(W)}{K_l(W)}. \tag{8.21}$$

It is convenient to define the normalized propagation constant as

$$b = \frac{\frac{\beta^2}{k_0^2} - n_2^2}{n_1^2 - n_2^2} = \frac{W^2}{V^2}. \tag{8.22}$$

Thus, $W = V\sqrt{b}$, and $U = V\sqrt{1-b}$. In terms of b, the eigenvalue Eq. (8.21) can be written as[2]

$$V\sqrt{1-b}\,\frac{J_{l-1}\left[V\sqrt{1-b}\right]}{J_l\left[V\sqrt{1-b}\right]} = -V\sqrt{b}\,\frac{K_{l-1}\left[V\sqrt{b}\right]}{K_l\left[V\sqrt{b}\right]} \qquad l \geq 1, \tag{8.23}$$

and

$$V\sqrt{1-b}\,\frac{J_1\left[V\sqrt{1-b}\right]}{J_0\left[V\sqrt{1-b}\right]} = V\sqrt{b}\,\frac{K_1\left[V\sqrt{b}\right]}{K_0\left[V\sqrt{b}\right]} \qquad l = 0. \tag{8.24}$$

For a given value of V, the solution of the preceding transcendental equations will give us discrete values of the normalized propagation constant b of the guided LP_{lm} modes. For a given value of l, there will be finite number of

solutions, and the m'th solution (m = 1, 2, 3, …) is referred to as the LP_{lm} mode. An interesting property of LP_{lm} modes is that one obtains universal curves describing the dependence of b (and therefore of U and W) on V. Further, since the modes are solutions of the scalar wave equation, they satisfy the orthonormality condition

$$\int_0^{\infty} \int_0^{2\pi} \psi_{lm}^{*}(r,\phi)\psi_{l'm'}(r,\phi)\, r\, dr\, d\phi = \delta_{ll'}\delta_{mm'}, \tag{8.25}$$

where $\delta_{mm'}$ is the Kronecker delta function.

8.3.2 Cutoff V values of LP_{lm} modes

It should be noted that a particular mode is possible only if the V value of the fiber is greater than a certain value, say, V_c, which is known as the *cutoff V value* of that mode. Physically, at the cutoff of a mode, the angle of incidence of the corresponding ray at the core–cladding interface is equal to the critical angle; hence,

$$\beta = k_0 n_2 \text{, i.e., } W = 0 \text{, giving } U = V_c. \tag{8.26}$$

Thus, the cutoff V values of LP_{lm} modes can be obtained by substituting $\beta = k_0 n_2$ [i.e., $W = 0$ and $U = V_c$ in Eqs. (8.23) and (8.24)], which is the m'th root of

(i) $$J_1(V_c) = 0,\ l = 0 \text{ modes,} \tag{8.27a}$$

(ii) $$J_0(V_c) = 0,\ l = 1 \text{ modes,} \tag{8.27b}$$

(iii) $$J_{l-1}(V_c) = 0,\ V_c \neq 0,\ l \geq 2 \text{ modes.} \tag{8.27c}$$

Using Eqs. (8.27a)–(8.27c), the cutoff V values of the first few LP_{lm} modes are given here: $LP_{01} \to 0.00$; $LP_{11} \to 2.4048$; LP_{02}, $LP_{21} \to 3.8317$.

Figure 8.3 gives the universal curves showing the variation of b with V for the few lower-order modes obtained from Eqs. (8.23) and (8.24). Using Eqs. (8.14) and (8.22), we see that guided modes are characterized by $0 < b < 1$. As can be seen, at a particular V value, the fiber can support only a finite number of modes.

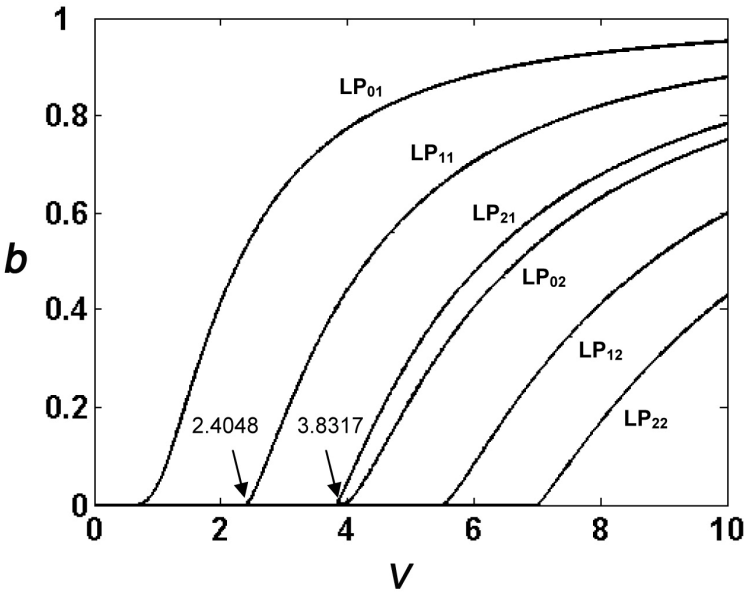


Figure 8.3 Variation of the normalized propagation constant *b* with normalized waveguide parameter *V* corresponding to a few lower-order modes. (Calculations courtesy of Ms. Triranjita Srivastava.)

8.4 Single-Mode Fiber

As is evident from Fig. 8.3, for a step-index fiber with $0 < V < 2.4048$, we will have only one guided mode—namely, the LP_{01} mode, also referred to as the *fundamental mode*. Such a fiber is referred to as a *single-mode fiber* (SMF) and is of tremendous importance in optical fiber communication systems. Polarization characteristics of optical fibers are also important, mainly only in the single-mode region. Since V depends on the operating wavelength, a given fiber may be single mode at one wavelength, while it may support more than one mode at another wavelength. The wavelength for which $V = 2.4048$ is known as the *cutoff wavelength* and is denoted by λ_c. Thus, a given fiber is single mode when $\lambda_0 > \lambda_c$. For a typical single-mode fiber (operating at 1550 nm), $a = 4.2$ μm, $n_2 = 1.444$ (for pure silica), and $\Delta = 0.0034$.

Example 8.1 As an example, we consider a step-index fiber with

$$n_2 = 1.447,\ \Delta = 0.003, \text{ and } a = 4.2\ \mu\text{m},$$

giving

$$V \simeq k_0 a n_2 \sqrt{2\Delta} = \frac{2.958}{\lambda_0},$$

where λ_0 is measured in μm. In this example, λ_c is given by

$$\frac{2.958}{\lambda_c} = 2.4048 \Rightarrow \quad \lambda_c = 1.23 \ \ \mu\text{m}.$$

Thus, for $\lambda_0 > 1.23$ μm, the fiber will be single mode.

8.4.1 Modal field pattern of the fundamental mode

The transverse dependence of the modal field of the fundamental mode is given by

$$\psi(r,\phi) = \begin{cases} \dfrac{A}{J_0(U)} J_0\left(\dfrac{Ur}{a}\right) & r < a \\ \dfrac{A}{K_0(W)} K_0\left(\dfrac{Wr}{a}\right) & r > a, \end{cases} \tag{8.28}$$

where U and W are determined by solving Eq. (8.24). For a single-mode step-index fiber, a convenient empirical formula for $b(V)$ is given by[5]

$$b(V) = \left(A - \frac{B}{V}\right)^2 \quad 1.5 \lesssim V \lesssim 2.5, \tag{8.29}$$

where $A \approx 1.1428$ and $B \approx 0.996$.

Table 8.1 gives the values of b as a function of V for the fundamental (LP_{01}) mode as obtained from Eqs. (8.24) and (8.29), respectively, for a step-index fiber.

Table 8.1 Values of b versus V of the LP_{01} mode for a step-index fiber.

V	b [by solving Eq. (8.24)]	b [using Eq. (8.29)]
1.5	0.229248	0.229249
1.6	0.270063	0.270712
1.7	0.309467	0.310157
1.8	0.347068	0.347471
1.9	0.382660	0.382653
2.0	0.416163	0.415767
2.1	0.447581	0.446911
2.2	0.476969	0.476200
2.3	0.504416	0.503754
2.4	0.530026	0.529693
2.5	0.553915	0.554131

Once b is known, one can calculate the propagation constant β using Eq. (8.22). Now, from Eq. (8.22),

$$b = \frac{\left(\frac{\beta}{k_0} - n_2\right)\left(\frac{\beta}{k_0} + n_2\right)}{(n_1 - n_2)(n_1 + n_2)}. \tag{8.30}$$

Since for a guided mode, β/k_0 lies between n_1 and n_2, and for all practical single-mode fibers, n_1 is very close to n_2, we may write Eq. (8.30) as

$$b \approx \frac{\frac{\beta}{k_0} - n_2}{n_1 - n_2}, \tag{8.31}$$

giving

$$\beta = \frac{\omega}{c}\left[n_2 + \left(n_1 - n_2\right) b\left(V\right)\right] = \frac{\omega}{c} n_2 (1 + \Delta b), \tag{8.32}$$

where we have used $\Delta = (n_1 - n_2) / n_2$.

Example 8.2 We consider a step-index fiber with $n_2 = 1.447$, $\Delta = 0.003$, and $a = 4.2$ μm, giving $V = 2.958/\lambda_0$, where λ_0 is measured in μm. Thus, for $\lambda_0 > 1.23$ μm, the fiber will be single mode. We assume an operating wavelength $\lambda_0 = 1.479$ μm so that $V = 2.0$, and therefore (from Table 8.1),

$$b \approx 0.4162 \;\Rightarrow\; \frac{\beta}{k_0} \approx n_2\,(1 + \Delta b) \approx 1.4488$$

$$\Rightarrow\; \beta \approx 6.1549 \times 10^6 \text{ m}^{-1}.$$

8.4.2 Spot size of the fundamental mode

The transverse field distribution associated with the fundamental mode of a single-mode fiber is an extremely important quantity, and it determines various important parameters, such as splice loss at joints between fibers, launching efficiencies from sources, and bending loss. For a step-index fiber, one obtains analytical expressions for the fundamental-mode field distribution in terms of Bessel functions [Eq. (8.28)]. For most single-mode fibers with a general transverse refractive index profile, the fundamental-mode field distribution can be well approximated by a Gaussian function, which can be written in the form

$$\psi(x, y) = A\, e^{-\frac{x^2+y^2}{w^2}} = A\, e^{-\frac{r^2}{w^2}}, \tag{8.33}$$

where w is referred to as the *Gaussian spot size* of the mode field pattern and $2w$ is called the *Gaussian mode field diameter* (MFD). MFD is a very important characteristic of a single-mode optical fiber. For a step-index fiber, one often uses the following empirical expression[6] for w:

$$\frac{w}{a} \approx 0.65 + \frac{1.619}{V^{3/2}} + \frac{2.879}{V^6} \qquad 0.8 \le V \le 2.5, \tag{8.34}$$

where a is the core radius. As an example, for the step-index fiber considered in the preceding examples and operating at 1300 nm, we have $V \approx 2.28$, giving $w \approx 4.8$ μm. Note that the spot size is larger than the core radius of the fiber; this is due to the penetration of the modal field into the cladding of the fiber. The same fiber will have a V value of 1.908 at $\lambda_0 = 1550$ nm, giving a value of the spot size ≈ 5.5 μm. *Thus, in general, the spot size increases with wavelength*. The standard single-mode fiber (SSMF) designated as G-652 fiber for operation at 1310 nm has an MFD of 9.2 ± 0.4 μm and an MFD of 10.4 ± 0.8 μm at 1550 nm.

For $2.4048 < V < 3.8317$, a step-index fiber supports two modes—namely, LP_{01} and LP_{11}—and the fiber is known as a two-mode fiber. For larger values of V (≥10), the fiber supports many modes and is known as a multimode fiber. Different modes (in a multimode fiber) travel with different group velocities, creating what is known as *intermodal dispersion*.

8.5 Pulse Dispersion in Single-Mode Optical Fibers

In digital communication systems, information to be sent is first coded in the form of pulses of light, and then these pulses are transmitted from the transmitter to the receiver, where the information is decoded. The larger the number of pulses that can be sent per unit time and remain resolvable at the receiver end, the larger the transmission capacity of the system. A pulse of light sent into a fiber broadens in time as it propagates through the fiber; this phenomenon is known as *pulse dispersion* (see Fig. 8.4). Pulse dispersion can occur for a variety of reasons. In the next section we will discuss the broadening of optical pulses due to the wavelength dependence of the refractive index of the fiber material, known as *material dispersion*.

8.5.1 Material dispersion

If β represents the propagation constant of the mode, the pulse will propagate through the fiber with what is known as the *group velocity* v_g, which is given by[7]

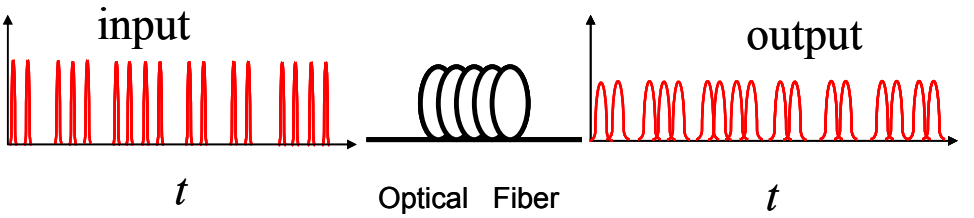


Figure 8.4 Schematic drawing of pulse dispersion: coded information in the form of light pulses is propagated through the optical fiber, where the pulses are attenuated and broadened in time.

$$v_g = \frac{1}{d\beta / d\omega}. \tag{8.35}$$

As most of the power carried by the mode is confined in the core, we assume that the pulse propagating through the fiber sees mainly the core of refractive index $n_1(\omega)$, and hence,

$$\beta(\omega) = \frac{\omega}{c} n_1(\omega). \tag{8.36}$$

Thus,

$$\frac{1}{v_g} = \frac{d\beta}{d\omega} = \frac{1}{c}\left[n_1(\omega) + \omega \frac{dn_1}{d\omega} \right]. \tag{8.37}$$

We may mention that it is customary to express $n(\omega)$ in terms of the free-space wavelength λ_0, which is related to ω through the equation

$$\omega = \frac{2\pi c}{\lambda_0}. \tag{8.38}$$

Thus,

$$\frac{dn_1}{d\omega} = \frac{dn_1}{d\lambda_0}\frac{d\lambda_0}{d\omega} = -\frac{\lambda_0^2}{2\pi c}\frac{dn_1}{d\lambda_0},$$

or

$$\frac{1}{v_g} = \frac{1}{c}\left[n_1(\lambda_0) - \lambda_0 \frac{dn_1}{d\lambda_0} \right]. \tag{8.39}$$

Thus, the time taken by a pulse to traverse a fiber length L is given by

$$\tau = \frac{L}{v_g} = \frac{L}{c}\left[n_1(\lambda_0) - \lambda_0 \frac{dn_1}{d\lambda_0} \right] . \tag{8.40}$$

Since its right-hand side depends on λ_0, Eq. (8.40) implies that different wavelengths will travel with different group velocities while propagating through a certain length of the fiber. Every source of light has a certain wavelength spread, which is often referred to as the *spectral width of the source*. For example, a white-light source (such as the sun) has a spectral width of about 300 nm; whereas, a light-emitting diode (LED) has a spectral width of about 25 nm, and a typical laser diode (LD) operating at 1300 nm has a spectral width of about 2 nm or less. Each wavelength component of the pulse travels with a slightly different group velocity and, in general, results in the broadening of the pulse. Thus, the pulse broadening is given by

$$\Delta\tau_m = \frac{d\tau}{d\lambda_0}\Delta\lambda_0 ,$$

or

$$\Delta\tau_m = -\frac{L\,\Delta\lambda_0}{c\,\lambda_0}\left[\lambda_0^2 \frac{d^2 n_1}{d\lambda_0^2} \right], \tag{8.41}$$

where L is the length of the fiber, $\Delta\lambda_0$ is the spectral width of the source, and c is the speed of light in free space. The subscript m in Eq. (8.41) signifies that we are considering material dispersion. We assume that

$$\Delta\lambda_0 = 1 \text{ nm} = 10^{-9} \text{ m} \text{ and } L = 1 \text{ km} = 1000 \text{ m} ,$$

and define the dispersion coefficient as

$$D_m = \frac{\Delta\tau_m}{L\Delta\lambda_0} \approx -\frac{1}{3\lambda_0}\left(\lambda_0^2 \frac{d^2 n_1}{d\lambda_0^2} \right) \times 10^4 \quad \text{ps/(nm} \cdot \text{km)} , \tag{8.42}$$

where λ_0 is measured in μm and we have assumed that c ≈ 3 × 10^8 m/s. The quantity D_m is usually referred to as the *material dispersion coefficient*. A medium is said to be characterized by positive dispersion when D_m is positive, and is said to be characterized by negative dispersion when D_m is negative.

For fused silica, which is the basic material used in optical fibers, an accurate empirical relation for refractive-index variation with wavelength, known as the *Sellmeier equation*, is given by[8]

$$n(\lambda_0) = C_0 + C_1\lambda_0^2 + C_2\lambda_0^4 + \frac{C_3}{(\lambda_0^2 - l)} + \frac{C_4}{(\lambda_0^2 - l)^2} + \frac{C_5}{(\lambda_0^2 - l)^3}, \quad (8.43)$$

where $C_0 = 1.4508554$, $C_1 = -0.0031268$, $C_2 = -0.0000381$, $C_3 = 0.0030270$, $C_4 = -0.0000779$, $C_5 = 0.0000018$, $l = 0.035$, and λ_0 is measured in μm. Using Eqs. (8.42) and (8.43), one can obtain the contribution of material dispersion in an optical fiber.

Example 8.3 In the first-generation optical communication systems, one used LEDs with $\lambda_0 \approx 0.85$ μm and $\Delta\lambda_0 \approx 25$ nm. At $\lambda_0 \approx 0.85$ μm, for pure silica,

$$\frac{d^2n}{d\lambda_0^2} \approx 0.030 \ (\mu\text{m})^{-2},$$

giving

$$D_m \approx -85 \text{ ps/(nm·km)},$$

the negative sign indicating that higher wavelengths travel faster than lower wavelengths. Thus, for $\Delta\lambda_0 \approx 25$ nm, the actual broadening of the pulse will be

$$\Delta\tau_m \approx 2.1 \text{ ns/km},$$

implying that, because of material dispersion, the pulse will broaden by 2.1 ns after traversing through 1 km of silica fiber.

Example 8.4 In the fourth-generation optical communication systems, one uses laser diodes at $\lambda_0 \approx 1.55$ μm with $\Delta\lambda_0 \approx 2$ nm. Now, at $\lambda_0 \approx 1.55$ μm,

$$\frac{d^2n}{d\lambda_0^2} \approx -0.0042 \ (\mu\text{m})^{-2},$$

giving

$$D_m \approx +21.7 \text{ ps/(nm·km)},$$

the positive sign indicating that higher wavelengths travel slower than lower wavelengths. Thus, for $\Delta\lambda_0 \approx 2$ nm, the actual broadening of the pulse will be

$$\Delta\tau_m \approx 43 \text{ ps/km},$$

implying that because of material dispersion, the pulse will broaden by 43 ps after traversing through 1 km of silica fiber.

8.5.2 Waveguide dispersion

As discussed earlier, because of the dependence of refractive index on wavelength, different wavelengths take different amounts of time to propagate along the fiber, which is known as *material dispersion*. We will show here that even if n_1 and n_2 are independent of wavelength (i.e., there is no material dispersion), the group velocity of a particular mode will depend on the wavelength. This leads to what is known as the *waveguide dispersion*.

Recall that β can be approximated [see Eq. (8.32)] as

$$\beta = \frac{\omega}{c} n_2 \left[1 + \Delta\, b(V)\right].$$

We assume that n_1 and n_2 are independent of ω and calculate group velocity:

$$\frac{1}{v_g} = \frac{d\beta}{d\omega} = \frac{1}{c} n_2 \left[1 + \Delta\, b(V)\right] + \frac{\omega}{c} n_2 \Delta \frac{db}{dV} \frac{dV}{d\omega}. \tag{8.44}$$

Now,
$$V = \frac{2\pi}{\lambda_0} a \sqrt{n_1^2 - n_2^2} = \frac{\omega}{c} a \sqrt{n_1^2 - n_2^2}\ . \tag{8.45}$$

Thus,
$$\frac{dV}{d\omega} = \frac{V}{\omega}, \tag{8.46}$$

and

$$\begin{aligned} \frac{1}{v_g} &= \frac{n_2}{c}\left[1 + \Delta\, b(V)\right] + \frac{n_2}{c} \Delta\, V \frac{db}{dV} \\ &= \frac{n_2}{c}\left[1 + \Delta \frac{d}{dV}(bV)\right]. \end{aligned} \tag{8.47}$$

Thus, the time taken by a pulse to traverse length L of the fiber is given by

$$\tau = \frac{L}{v_g} = \frac{L}{c} n_2 \left[1 + \Delta \frac{d}{dV}(bV)\right]. \tag{8.48}$$

From Eq. (8.48), we see that even if n_1 and n_2 are independent of wavelength, the group velocity (and hence τ) will still depend on ω because of the dependence of b on V (see Fig. 8.3). This leads to what is known as the *waveguide dispersion*. Physically, waveguide dispersion arises due to the fact that the spot size depends

on the wavelength. For a source having a spectral width $\Delta\lambda_0$, the corresponding waveguide dispersion is given by

$$\Delta\tau_{\mathrm{w}} = \frac{d\tau}{d\lambda_0}\Delta\lambda_0 \cong \frac{L}{c} n_2 \Delta \frac{d^2}{dV^2}(bV)\frac{dV}{d\lambda_0}\Delta\lambda_0 . \tag{8.49}$$

From Eq. (8.45), we find that

$$\frac{dV}{d\lambda_0} = -\frac{V}{\lambda_0}. \tag{8.50}$$

Thus,
$$\Delta\tau_{\mathrm{w}} = -\frac{L n_2 \Delta}{c} f(V)\frac{\Delta\lambda_0}{\lambda_0}. \tag{8.51}$$

The corresponding dispersion coefficient is defined as

$$D_{\mathrm{w}} = \frac{\Delta\tau_{\mathrm{w}}}{L\Delta\lambda_0} = -\frac{n_2\Delta}{c\lambda_0} f(V), \tag{8.52}$$

where
$$f(V) \equiv V\frac{d^2}{dV^2}(bV). \tag{8.53}$$

For a step-index fiber, b as a function of V is a universal curve; therefore, the variation of $f(V)$ with V will also be universal. A convenient empirical formula for a step-index fiber is given by[9]

$$f(V) \approx 0.080 + 0.549(2.834 - V)^2 \quad 1.3 < V < 2.4. \tag{8.54}$$

Using the preceding equation, the empirical expression for waveguide dispersion in step-index fibers is

$$D_{\mathrm{w}} = -\frac{n_2\Delta}{3\lambda_0} \times 10^4 \left[0.080 + 0.549(2.834 - V)^2\right] \ \mathrm{ps/(nm\cdot km)}, \tag{8.55}$$

where λ_0 is measured in μm.

Thus, the total dispersion in the case of a single-mode optical fiber can be attributed to two types of dispersion—namely, material dispersion and waveguide dispersion. Indeed, it can be shown that in most single-mode fibers, the total dispersion coefficient D_{tot} is given to a good accuracy by the sum of material D_{m} and waveguide D_{w} dispersion coefficients. The material contribution

is given by Eq. (8.42), while the waveguide contribution for a step-index fiber is given by Eq. (8.55).

In the single-mode regime, the quantity within the bracket in Eq. (8.55) is usually positive; hence, the waveguide dispersion is negative. Since the sign of material dispersion depends on the operating wavelength region, it is possible that the two effects—namely, material dispersion and waveguide dispersion—cancel each other at a certain wavelength. Such a wavelength, which is a very important parameter of single-mode fibers, is referred to as the *zero-dispersion wavelength* λ_{ZD}. Single-mode step-index optical fibers that have a zero-dispersion wavelength around 1300 nm are known as *standard single-mode fibers* (SSMFs) or G-652 fibers. These fibers have been used extensively in optical communication systems.

In Fig. 8.5, we show the wavelength dependence of D_m, D_w, and D_{tot} for a typical SSMF with parameters as given in Example 8.2. The variation of D_m is calculated using Eqs. (8.42) and (8.43) and that of D_w using Eq. (8.55). The figure shows that the total dispersion passes through zero around $\lambda_0 = 1300$ nm.

8.5.3 Dispersion-shifted fibers

It may be noted from Eq. (8.55) that the waveguide dispersion depends on the fiber parameters, which can be selected to make the total dispersion zero at some desired wavelength. Because the lowest loss in an optical fiber occurs at a wavelength of 1550 nm and optical amplifiers are also available in the 1550-nm window, fiber designs can be modified to shift the zero-dispersion wavelength to the 1550-nm wavelength window. As an example, we consider a step-index single-mode fiber with parameters as

$$n_2 = 1.444,\ \Delta = 0.0075, \text{ and } a = 2.3\ \mu\text{m, giving } V = 2.556/\lambda_0,$$

where λ_0 is measured in μm. Using the preceding parameters in Eq. (8.55), at $\lambda_0 =$ 1550 nm one obtains

$$D_w \approx -20 \text{ ps/(nm·km)}.$$

On the other hand, using Eqs. (8.42) and (8.43), the material dispersion at this wavelength is

$$D_m \approx +20 \text{ ps/(nm·km)}.$$

This shows that for the considered fiber parameters, the total dispersion is zero at $\lambda_0 = 1550$ nm. The corresponding variation of D_m, D_w, and D_{tot} with wavelength is shown in Fig. 8.6. The preceding example shows that one can shift the zero dispersion wavelength to a suitable value by changing the fiber parameters. Such fibers are referred to as *dispersion-shifted fibers* (DSFs) when dispersion is zero around 1550 nm and *nonzero-dispersion-shifted fibers* (NZDSFs) when dispersion is finite but small around 1550 nm.

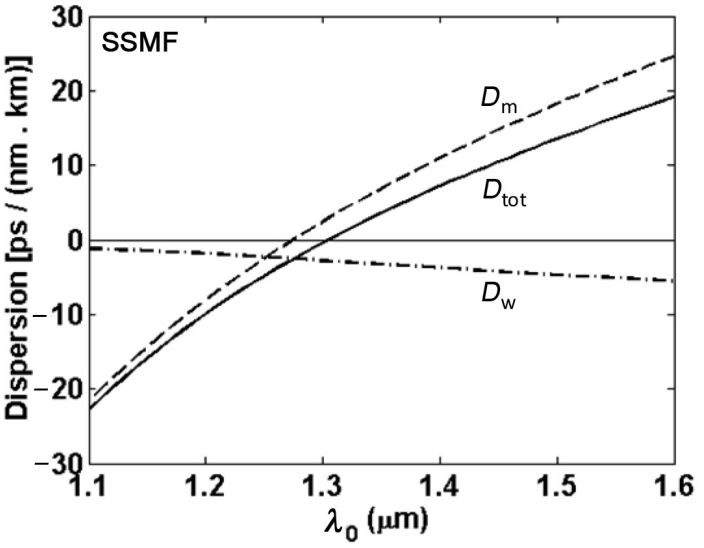


Figure 8.5 The wavelength dependence of D_m, D_w, and D_{tot} for a typical conventional SSMF with parameters given in Example 8.2, showing $\lambda_{ZD} \approx 1300$ nm. (Calculations courtesy of Ms. Triranjita Srivastava.)

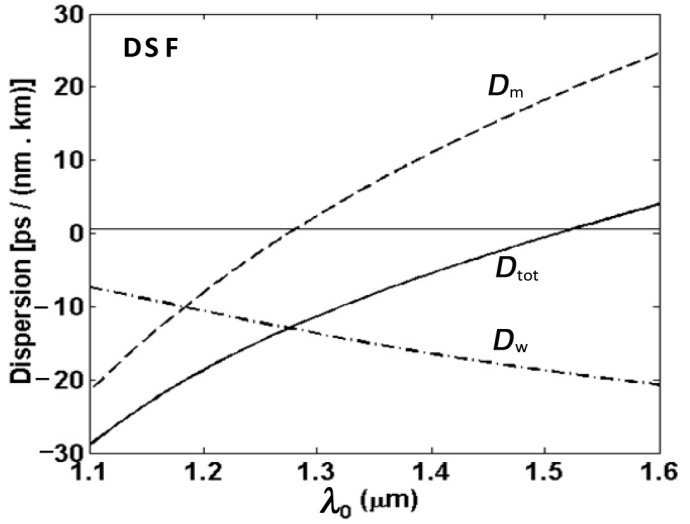


Figure 8.6 The wavelength dependence of D_m, D_w, and D_{tot} for a typical dispersion-shifted fiber with parameters as $n_2 = 1.444$, $\Delta = 0.0075$, and $a = 2.3$ μm. The zero-dispersion wavelength is around 1550 nm. (Calculations courtesy of Ms. Triranjita Srivastava.)

8.6 Polarization Characteristics of Single-Mode Fibers

The discussion and the numerical results presented in the preceding sections use LP_{lm} modes, which are extremely accurate for practical optical fibers, as $n_1 \approx n_2$.

In this approximation, various modes are linearly polarized. The exact modes, obtained by satisfying the exact boundary conditions at the core–cladding interface, however, are not perfectly linearly polarized. In the following section, we briefly discuss the exact vector modes of a step-index fiber.

8.6.1 Exact vector modes of a step-index fiber

In a step-index fiber, both core and cladding regions are homogeneous, and hence, as discussed in Section 2.2, the field components E_z and H_z in each region will satisfy the following wave equations:

$$\nabla^2 E_z = \varepsilon \mu \frac{\partial^2 E_z}{\partial t^2}, \tag{8.56a}$$

and

$$\nabla^2 H_z = \varepsilon \mu \frac{\partial^2 H_z}{\partial t^2}. \tag{8.56b}$$

Keeping the cylindrical geometry of the fiber in mind, we solve these equations in cylindrical coordinates $(r, \phi, \text{and } z)$; z being parallel to the fiber axis and also taken as the direction of propagation. We first solve the preceding equations for E_z and H_z. Since the refractive index of the fiber does not depend on the z coordinate, we can assume E_z and H_z to be of the form

$$\begin{aligned} \mathbf{E}(r,\phi,z,t) &= \mathbf{E}(r,\phi)\,\mathrm{e}^{i(\omega t-\beta z)} \\ \mathbf{H}(r,\phi,z,t) &= \mathbf{H}(r,\phi)\,\mathrm{e}^{i(\omega t-\beta z)}, \end{aligned} \tag{8.57}$$

where β represents the propagation constant of the mode. Substituting the preceding expressions into Maxwell's Eqs. (2.11) and (2.12) written in cylindrical coordinates, we can show[4,10] that the other field components E_r, E_ϕ, H_r, and H_ϕ are given by

$$\begin{aligned} E_r &= -\frac{i}{\alpha^2}\left(\beta\frac{\partial E_z}{\partial r} + \omega\mu\frac{1}{r}\frac{\partial H_z}{\partial \phi}\right), \\ E_\phi &= -\frac{i}{\alpha^2}\left(\beta\frac{1}{r}\frac{\partial E_z}{\partial \phi} - \omega\mu\frac{\partial H_z}{\partial r}\right), \\ H_r &= -\frac{i}{\alpha^2}\left(\beta\frac{\partial H_z}{\partial r} - \omega\varepsilon\frac{1}{r}\frac{\partial E_z}{\partial \phi}\right), \\ H_\phi &= -\frac{i}{\alpha^2}\left(\beta\frac{1}{r}\frac{\partial H_z}{\partial \phi} + \omega\varepsilon\frac{\partial E_z}{\partial r}\right), \end{aligned} \tag{8.58}$$

where $\alpha^2 = k_0^2 n^2(r) - \beta^2$ and $k_0^2 = \omega^2 \varepsilon_0 \mu_0$. Thus, all of the field components are known once E_z and H_z are known. Substituting E_z and H_z from Eq. (8.57) into Eqs. (8.56a) and (8.56b), one can easily show that $E_z(r,\phi)$ and $H_z(r,\phi)$ satisfy the following equation:

$$\frac{\partial^2 \psi}{\partial r^2} + \frac{1}{r}\frac{\partial \psi}{\partial r} + \frac{1}{r^2}\frac{\partial^2 \psi}{\partial \phi^2} + \left[k_0^2 n^2(r) - \beta^2\right]\psi = 0, \tag{8.59}$$

where $\psi(r,\phi)$ represents $E_z(r,\phi)$ or $H_z(r,\phi)$. As discussed in Section 8.3, Eq. (8.59) can be solved by using the method of separation of variables, and for the guided modes, the well-behaved solutions are given by

$$\psi(r,\phi) = \begin{cases} \dfrac{A}{J_l(U)} J_l\left(\dfrac{Ur}{a}\right)\begin{bmatrix}\cos l\phi \\ \sin l\phi\end{bmatrix} & r < a, \\ \dfrac{A}{K_l(W)} K_l\left(\dfrac{Wr}{a}\right)\begin{bmatrix}\cos l\phi \\ \sin l\phi\end{bmatrix} & r > a, \end{cases} \tag{8.60}$$

where A is a constant, and U and W are the same, as defined in Eq. (8.17). In Eq. (8.60), we have already implemented the continuity of E_z and H_z at $r = a$.

Having determined the E_z and H_z components, the other field components can be determined by using Eq. (8.58). It should be mentioned here that the ϕ dependence of E_r, E_ϕ, H_r, and H_ϕ should also be of the $\cos l\phi$ or $\sin l\phi$ type. This requires that if the ϕ dependence of E_z is the $\cos l\phi$ ($\sin l\phi$) type, the ϕ dependence of H_z should be the $\sin l\phi$ ($\cos l\phi$) type [see Eq. (8.58)]. Thus,

$$E_z(r,\phi) = \begin{cases} \dfrac{A}{J_l(U)} J_l\left(\dfrac{Ur}{a}\right)\begin{bmatrix}\cos l\phi \\ \sin l\phi\end{bmatrix} & r < a, \\ \dfrac{A}{K_l(W)} K_l\left(\dfrac{Wr}{a}\right)\begin{bmatrix}\cos l\phi \\ \sin l\phi\end{bmatrix} & r > a, \end{cases} \tag{8.61}$$

$$H_z(r,\phi) = \begin{cases} \dfrac{B}{J_l(U)} J_l\left(\dfrac{Ur}{a}\right)\begin{bmatrix}\sin l\phi \\ \cos l\phi\end{bmatrix} & r < a, \\ \dfrac{B}{K_l(W)} K_l\left(\dfrac{Wr}{a}\right)\begin{bmatrix}\sin l\phi \\ \cos l\phi\end{bmatrix} & r > a. \end{cases} \tag{8.62}$$

Substituting $E_z(r,\phi)$ and $H_z(r,\phi)$ in Eq. (8.58), one obtains E_r, E_ϕ, H_r, and H_ϕ in the core as well as the cladding regions. If we make E_ϕ and H_ϕ continuous at $r = a$, we obtain the following two equations:[4]

$$A\beta\left[\frac{1}{U^2}+\frac{1}{W^2}\right]l = -B\omega\mu_0\left[\frac{J_l'(U)}{UJ_l(U)}+\frac{K_l'(W)}{WK_l(W)}\right], \tag{8.63}$$

and

$$A\omega\varepsilon_0\left[n_1^2\frac{J_l'(U)}{UJ_l(U)}+n_2^2\frac{K_l'(W)}{WK_l(W)}\right] = -B\beta\left[\frac{1}{U^2}+\frac{1}{W^2}\right]l. \tag{8.64}$$

Dividing Eq. (8.64) by Eq. (8.63), we obtain

$$\left[\frac{J_l'(U)}{UJ_l(U)}+\frac{K_l'(W)}{WK_l(W)}\right]\left[n_1^2\frac{J_l'(U)}{UJ_l(U)}+n_2^2\frac{K_l'(W)}{WK_l(W)}\right] = \frac{\beta^2}{k_0^2}\left[\frac{1}{U^2}+\frac{1}{W^2}\right]^2 l^2. \tag{8.65}$$

The preceding transcendental equation is the exact eigenvalue equation whose solutions give the propagation constants of various guided modes of a step-index fiber. The modes are, in general, hybrid modes consisting of all of the six field components except for $l = 0$. In the case where $l = 0$, Eq. (8.65) is further divided into the following two equations:

TE modes:
$$\frac{J_0'(U)}{UJ_0(U)} + \frac{K_0'(W)}{WK_0(W)} = 0, \tag{8.66}$$

TM modes:
$$n_1^2\frac{J_0'(U)}{UJ_0(U)} + n_2^2\frac{K_0'(W)}{WK_0(W)} = 0. \tag{8.67}$$

Note that when Eq. (8.66) is satisfied, from Eq. (8.63), $A = 0$, implying that $E_z = 0$. This means that for such modes, the longitudinal component of the electric field is zero, and hence, the modes are known as *transverse electric* (*TE*) *modes*. Similarly, when Eq. (8.67) is satisfied, from Eq. (8.64), $B = 0$, implying that $H_z = 0$. Thus, for such modes, the longitudinal component of the magnetic field is zero, and hence, the modes are known as *transverse magnetic* (*TM*) *modes*.

For $l \geq 1$, as mentioned earlier, the modes are hybrid modes consisting of all of the six field components. The propagation constants of these modes are obtained by solving Eq. (8.65), which results in two types of modes designated as HE and EH modes. In the following section, we derive the eigenvalue equations of HE and EH modes in the weakly guiding approximation ($\Delta << 1$).

8.6.1.1 Eigenvalue equations of HE and EH modes for $\Delta << 1$

We first put β^2 in terms of U^2 and W^2 in Eq. (8.65). Using the definitions of U and W [Eq. (8.17)], we can write

$$\frac{k_0^2 n_1^2 - \beta^2}{U^2} = \frac{\beta^2 - k_0^2 n_2^2}{W^2},$$

i.e,

$$\frac{\beta^2}{k_0^2}\left[\frac{1}{U^2} + \frac{1}{W^2}\right] = \left[\frac{n_1^2}{U^2} + \frac{n_2^2}{W^2}\right]. \tag{8.68}$$

Using the preceding expression in Eq. (8.65), the eigenvalue equation can be recast as

$$\left[\frac{J_l'(U)}{UJ_l(U)} + \frac{K_l'(W)}{WK_l(W)}\right]\left[n_1^2 \frac{J_l'(U)}{UJ_l(U)} + n_2^2 \frac{K_l'(W)}{WK_l(W)}\right] = l^2 \left[\frac{1}{U^2} + \frac{1}{W^2}\right]\left[\frac{n_1^2}{U^2} + \frac{n_2^2}{W^2}\right]. \tag{8.69}$$

If we take the limit $n_1 \to n_2$, the preceding equation gives the following pair of equations:

$$\left[\frac{J_l'(U)}{UJ_l(U)} + \frac{K_l'(W)}{WK_l(W)}\right] = \pm l \left[\frac{1}{U^2} + \frac{1}{W^2}\right]. \tag{8.70}$$

The equation resulting in the positive term on the right-hand side in the preceding equation belongs to the EH mode, and the equation resulting in the negative term on the right-hand side belongs to the HE mode. Using the following recurrence relations of Bessel functions given in Eqs. (8.20a) and (8.20b), Eq. (8.70) can be rewritten as

EH modes:
$$\frac{J_{l+1}(U)}{UJ_l(U)} = -\frac{K_{l+1}(W)}{WJ_l(W)}, \tag{8.71}$$

HE modes:
$$\frac{J_{l-1}(U)}{UJ_l(U)} = +\frac{K_{l-1}(W)}{WK_l(W)}. \tag{8.72}$$

It may be mentioned here that for a given value of l, there may be several possible solutions, and the m'th solution of each equation is denoted as the EH_{lm} and HE_{lm} mode, respectively.

8.6.1.2 Cutoff conditions of the various modes

As discussed earlier, the cutoff V values of various guided modes can be obtained from the eigenvalue Eq. (8.65) by substituting the values of Bessel functions in the limit: $\beta = k_0 n_2$, i.e., $W = 0$ and $U = V_c$. The cutoffs of different modes are the various roots[10] of

(i) $$J_0(V_c) = 0, \text{ TE}_{0m} \text{ and TM}_{0m} \text{ modes } (l = 0), \tag{8.73}$$

(ii) $$J_1(V_c) = 0, \text{ HE}_{lm} \text{ mode } (l = 1), \tag{8.74}$$

$$\left(\frac{n_1^2}{n_2^2} + 1\right) J_{l-1}(V_c) = \frac{V_c}{l-1} J_l(V_c), \text{ HE}_{lm} \text{ mode } (l \geq 2). \tag{8.75a}$$

In the limit $n_1 \to n_2$, the preceding equation reduces to

$$J_{l-2}(V_c) = 0, \tag{8.75b}$$

(iii) $$J_l(V_c) = 0, \; V_c \neq 0 \text{ EH}_{lm} \text{ mode.} \tag{8.76}$$

Using the preceding equations, we arrange below the first few modes according to the increasing cutoff V values:

0.000	HE_{11}
2.4048	TE_{01}, TM_{01}, and HE_{21}
3.8317	HE_{12} and EH_{11}.

(Note that the cutoff of the HE_{21} mode is obtained in the limit $n_1 \to n_2$, i.e., from Eq. (8.75b). The exact value depends on n_1/n_2 [see Eq. (8.75a)] and is slightly higher than 2.4048.) In the limit $n_1 \to n_2$, these vector modes are converted to LP_{lm} modes; the correspondence between the two modes is given by[4]

$$\begin{aligned} &LP_{0m} = HE_{1m} \\ &LP_{1m} = TE_{0m}, TM_{0m}, HE_{2m} \\ &LP_{lm} = HE_{l+1,m}, EH_{l-1,m} \; (l \geq 2). \end{aligned} \tag{8.77}$$

The most important observation here is that the HE_{11} mode has zero cutoff and hence exists at all frequencies. As the V parameter increases and approaches 2.4048, the next higher-order modes (TE_{01}, TM_{01}) will also be supported. Thus, the single-mode region is again given by the condition $0 < V < 2.4048$. If this condition is satisfied, the fiber will support only one mode—namely, the HE_{11} mode.

The so-called single-mode fibers, in fact, support two orthogonally polarized modes, propagating with propagation constants β_x and β_y, respectively. Figure 8.7 schematically depicts the polarization states of these two fundamental vector modes—namely, HE_{11}^{x} and HE_{11}^{y}.

It may be noted that that the HE_{11}^{x} or HE_{11}^{y} mode is predominantly x or y polarized, having also a tiny y or x component. Under ideal conditions, circular-core optical fibers have no birefringence, i.e., ($\beta_x = \beta_y$). However, practical fibers do not have a perfectly circular core. As a result, the two modes have slightly different propagation constants ($\beta_x \neq \beta_y$), and the fiber becomes birefringent. The birefringence is measured in terms of B or Δn_{eff}, defined as

$$B = \beta_x - \beta_y \qquad \text{or} \qquad \Delta n_{\mathrm{eff}} = B / k_0 .$$

Apart from core ellipticity, many other factors can introduce birefringence in the fiber. In Section 8.6.2, we discuss the various origins of birefringence in optical fibers.

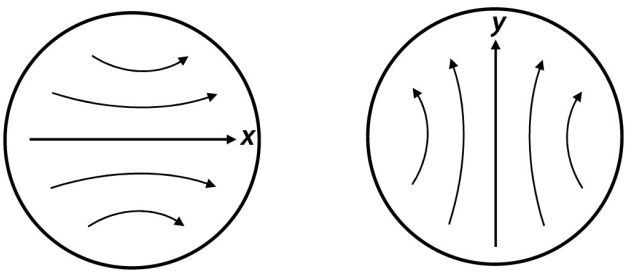
8.6.2 Origins of birefringence in optical fibers

The various reasons that an optical fiber may become birefringent are shown in Fig. 8.8 and are discussed in the remainer of this chapter.

8.6.2.1 Core ellipticity

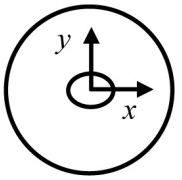
The geometrical anisotropy due to core ellipticity [Fig. 8.8(a)] introduces a linear birefringence in the fiber. For fibers with small core ellipticity, the birefringence near the first higher-mode cutoff is approximately given by[11]

$$B_{\mathrm{ce}} = (\beta_x - \beta_y) \approx 0.2 k_0 \left(\frac{a}{b} - 1 \right) (\Delta n)^2 , \tag{8.78}$$

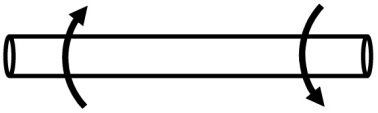


HE_{11}^{x} HE_{11}^{y}

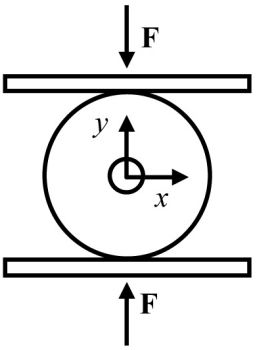
Figure 8.7 Schematic of polarization states for orthogonally polarized HE_{11}^{x} and HE_{11}^{y} modes.



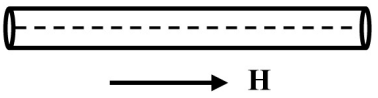
(a) Core ellipticity



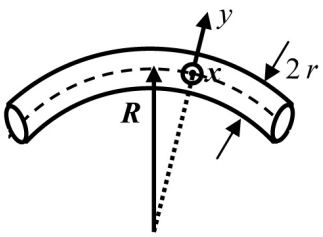
(d) Twist



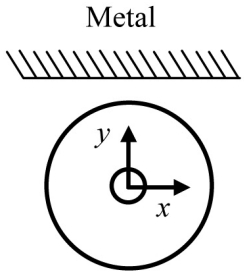
(b) Lateral stress



(e) Axial magnetic field



(c) Bend



(f) Metal Layer

Figure 8.8 Various mechanisms that produce birefringence in an optical fiber.

where $k_0 = 2\pi / \lambda_0$ (λ_0 being the free-space wavelength), Δn is the core and cladding refractive index difference, and a and b represent the semi-major and semi-minor axes of the core ellipse. In Eq. (8.78), β_x and β_y represent the propagation constants of the x- and y-polarized modes, where the x and y axes are taken parallel to the major and minor axis, respectively.

Equation (8.78) indicates that the birefringence is higher in fibers with larger core ellipticity and higher core and cladding refractive index difference. A positive value of B_{ce} means that the *x* component travels as a slow component. The corresponding difference between the effective indices of the slow and fast components is thus given by

$$\Delta n_{\text{eff}} = \frac{B_{\text{ce}}}{k_0} \approx 0.2\left(\frac{a}{b}-1\right)(\Delta n)^2 . \tag{8.79}$$

Example 8.5 We consider a single-mode optical fiber with $\Delta n = 0.005$ and core ellipticity of 1%, i.e., $(a/b-1) = 0.01$. Equation (8.79) gives $\Delta n_{\text{eff}} = 5\times10^{-8}$. Core ellipticity is also responsible for asymmetrical stresses developed in the fiber core. These stresses generate an extra birefringence, which is discussed in the next chapter.

8.6.2.2 Lateral stress

An asymmetrical lateral stress on the fiber also produces linear birefringence in the fiber via a strain-optic effect. If the fiber is pressed (for instance, along the *y* axis) between two parallel plates [see Fig. 8.8(b)], the generated birefringence is given by[11,12]

$$B_{\text{s}} = (\beta_x - \beta_y) = -k_0\, h \frac{F}{r}, \tag{8.80}$$

with

$$h = \frac{2\, n^3}{\pi}\frac{(1+\nu)}{E}\left(p_{11}-p_{12}\right). \tag{8.81}$$

Here, n is the average refractive index of the fiber core and cladding, p_{11} and p_{12} are the components of the strain optical tensor, E is the Young's modulus, and ν is the Poisson's ratio of the fiber material. Further, r represents the outer radius (including the cladding) of the fiber, which for a standard fiber is 62.5 μm, and F represents the lateral force per unit length of the fiber in kg/m.

Taking n = 1.46, p_{11} = 0.12, p_{12} = 0.27, $E = 7.75 \times 10^9$ kg/m^2, and $\nu = 0.17$ for fused silica, the difference between the effective indices of the lateral-stress-induced slow and fast components is

$$\Delta n_{\text{eff}} = \frac{B_{\text{s}}}{k_0} = 4.48\times10^{-11}\left(\frac{F}{r}\right). \tag{8.82}$$

Example 8.6 Substituting F = 1 gm/cm, i.e., 0.1 kg/m, and $r = 62.5\times10^{-6}$ m in Eq. (8.82), one obtains $\Delta n_{\text{eff}} \approx 7\times10^{-8}$.

8.6.2.3 Bending

Bending of a fiber introduces different types of stresses in the outer and inner portion of the fiber, leading to a linear birefringence, which for silica fibers is given by[13]

$$B_{\mathrm{b}} = (\beta_x - \beta_y) = -k_0 \frac{n^3}{4}(1+\nu)\left(p_{11} - p_{12}\right)\left(\frac{r}{R}\right)^2 \text{ rad/m}, \qquad (8.83)$$

where R represents the bend radius. In the preceding equation, the x axis is taken perpendicular to the plane of bending and the y axis in the plane of bending [Fig. 8.8(c)]. Substituting $n = 1.46$, $p_{11} = 0.12$, $p_{12} = 0.27$, and $\nu = 0.17$ in Eq. (8.83), for fused silica, the difference between the effective indices of the bending-induced slow and fast components is

$$\Delta n_{\mathrm{eff}} = \frac{B_{\mathrm{b}}}{k_0} = 0.136\left(\frac{r}{R}\right)^2. \qquad (8.84)$$

Example 8.7 Substituting R = 10 cm, i.e., 0.1 m, and $r = 62.5\times10^{-6}$ m in Eq. (8.84), one obtains $\Delta n_{\mathrm{eff}} \approx 5.3\times10^{-8}$. Bending-induced birefringence is used to fabricate in-line fiber optic wave plates to control the polarization state of the guided light, as discussed in the next chapter.

8.6.2.4 Twists

A twist [Fig. 8.8(d)] in the fiber produces a circular birefringence, given by[14]

$$B_{\mathrm{t}} = (\beta_{\mathrm{rc}} - \beta_{\mathrm{lc}}) = g\tau \text{ rad/m}, \qquad (8.85)$$

where β_{rc} and β_{lc} represent the propagation constants of the right-circularly and left-circularly polarized modes, respectively, $g = -n^2/2\left(p_{11} - p_{12}\right) \approx 0.16$ for silica fibers, and τ is the twist rate (in rad/m). Thus, a linearly polarized light will be rotated along a twisted fiber with a rotation rate given by

$$\alpha = \frac{1}{2} g\tau \text{ rad/m}. \qquad (8.86)$$

A positive value of g means that if the twist is counterclockwise (with respect to an observer looking against the direction of propagation), the previously mentioned rotation will also be counterclockwise (i.e., the left-circular component will be faster). Thus, the difference between the effective indices of the twist-induced slow and fast components is given by

$$\Delta n_{\text{eff}} = (n_{\text{rc}} - n_{\text{lc}}) = \frac{B_{\text{b}}}{k_0} = \frac{\lambda_0}{2\pi} g\tau \,. \tag{8.87}$$

Example 8.8 A twist of 1 turn/m in a fiber at $\lambda_0 = 1.5\,\mu\text{m}$ will produce

$$\Delta n_{\text{eff}} = \frac{1.5\times 10^{-6}}{2\pi} \times 0.16 \times 2\pi = 2.4\times 10^{-7} \,.$$

8.6.2.5 Magnetic field

A longitudinal (i.e., axial) magnetic field **H** [Fig. 8.8(e)] produces a circular birefringence in the fiber via the Faraday effect and is given by[15]

$$B_{\text{H}} = \beta_{\text{rc}} - \beta_{\text{lc}} = \frac{2V_{\text{d}}}{l} \int \mathbf{H} \bullet \mathbf{dl} \,, \tag{8.88}$$

where l represents the length of the fiber, and the line integral is taken along the direction of propagation. Further, V_{d} is the Verdet constant of the material and is equal to 4.7×10^{-6} rad/A for silica fibers.

It should be noted that unlike in the previous cases, the sign of birefringence produced by an axial magnetic field depends on the direction of propagation relative to **H**. If the wave is propagating along **H**, then $\beta_{\text{rc}} > \beta_{\text{lc}}$ (left handed), and if the wave is propagating opposite to **H**, then $\beta_{\text{rc}} < \beta_{\text{lc}}$ (right handed). An important property of the Faraday effect is that it is nonreciprocal, which means that if light propagating in one direction undergoes rotation θ, light propagating in the opposite direction undergoes rotation $-\theta$. This property is exploited in realizing important polarization components such as optical isolators and circulators. In a constant magnetic field of magnitude H, birefringence produced by an axial magnetic field is given by

$$\left|B_{\text{H}}\right| = 2V_{\text{d}} H \text{ rad/m.} \tag{8.89}$$

Thus, an axial magnetic field of magnitude H A/m will rotate the plane of polarization of the guided wave with a rate of

$$\alpha = V_{\text{d}} H \text{ rad/m.} \tag{8.90}$$

Example 8.9 An axial magnetic field of magnitude 1 A/m will generate a birefringence of 9.4×10^{-6} rad/m; thus, the polarization ellipse of a propagating polarized beam will rotate with a rate of 4.7×10^{-6} rad/m along the fiber. One of the important applications of the Faraday effect is in the measurement of electric currents using optical fibers, as discussed in the next chapter.

8.6.2.6 Metal layer near the fiber core

A dielectric–metal interface supports a TM-polarized surface wave (i.e., an electric field perpendicular to the interface), known as a surface plasmon polariton (SPP). Thus, if an optical fiber is side polished up to near its core and a metal layer is deposited on it [Fig. 8.8(f)], the fiber becomes birefringent. The TE (x-polarized) and the TM (y-polarized) modes propagate with different propagation constants and loss coefficients. Depending on the metal, the distance (from the core), and the thickness of the metal layer, the TM mode may be highly lossy due to coupling between the fiber mode and the SPP supported by the dielectric–metal interface. This mechanism is used to realize efficient in-line fiber polarizers and many biochemical sensors.

It may be mentioned that a deliberate and controlled birefringence introduced in a fiber can be used to realize several in-line fiber components and devices. In the next chapter, we will discuss some applications of birefringence in optical fibers. On the other hand, a random and uncontrolled birefringence in a fiber causes many problems, as is discussed in Chapter 10.

References

1. T. Miya, Y. Terunama, T. Hosaka, and T. Miyasita, "An ultimate low loss single mode fiber at 1.55 μm," *Electron. Lett.* **15**, 106–108 (1979).
2. A. Ghatak and K. Thyagarajan, *Optical Electronics*, Cambridge University Press, New York (1989).
3. A. Ghatak and K. Thyagarajan, *Introduction to Fiber Optics*, Cambridge University Press, Cambridge, UK (1998).
4. K. Okamota, *Fundamentals of Optical Waveguides*, Academic Press, San Diego, CA (2000).
5. H. D. Rudolph and E. G. Neumann, "Approximation for the eigenvalues of the fundamental mode of a step index glass fiber waveguide," *Nachrichtentech*. Z. **4**, 328–329 (1976).
6. D. Marcuse, "Loss analysis of single mode fiber splices," *Bell Syst. Tech. J.* **56**, 703–718 (1977).
7. A. Ghatak, *Optics*, McGraw-Hill, New York (2009).
8. U. C. Paek, G. E. Peterson, and A. Carnevale, "Dispersionless single mode light guides with α index profiles," *Bell Syst. Tech. J.* **60**, 583–598 (1981).
9. D. Marcuse, "Interdependence of waveguide and material dispersion," *Appl. Opt*. **18**, 2930–2932 (1979).
10. D. Marcuse, *Light Transmission Optics*, 2nd ed., Van Nostrand Reinhold Co., New York (1982).
11. S. C. Rashleigh, "Origins and control of polarization effects in single-mode fibers," *J. Lightw. Technol.* **1**, 312–331 (1983).

12. D. N. Payne, A. J. Barlow, and J. J. R. Hansen, "Development of low and high-birefringence optical fibers," *IEEE J. Quantum Electron.* **18**, 477–488 (1982).
13. R. Ulrich, S. C. Rashleigh, and W. Eickhoff, "Bending-induced birefringence in single-mode fibers," *Opt. Lett.* **5,** 273–275 (1980).
14. R. Ulrich and A. Simon, "Polarization optics of twisted single-mode fibers," *Appl. Opt.* **18**, 2241–2251 (1979).
15. A. M. Smith, "Polarization and magneto-optical properties of single-mode fibers," *Appl. Opt.* **17**, 52–56 (1978).

Bibliography

Ghatak, A., I. C. Goyal, and R. Varshney, *FIBER OPTICA: A Software for Characterizing Fiber and Integrated-Optic Waveguides*, Viva Books, New Delhi (1999).

Gloge, D., "Weakly guiding fibers," *Appl. Opt.* **10**, 2252–2258 (1971).

Marcuse, D., "Gaussian approximation of the fundamental modes of graded index fibers," *J. Opt. Soc. Am.* **68**, 103–109 (1978).

Mynbaev, D. K. and L. L. Scheiner, *Fiber-Optic Communications Technology*, Prentice Hall, Upper Saddle River, NJ (2001).

Snyder, A. W. and J. D. Love, *Optical Waveguide Theory*, Chapman & Hall, London (1983).